# Finite Element Analysis of BAW Sensor

M. Hashiguchi*[1] and Y. Sumiyoshi[1]
[1]Keisoku Engineering System Co.,Ltd.
*1-9-5 Uchikanda, Chiyoda-ku, Tokyo, 101-0047 Japan, info@kesco.co.jp

**Abstract:** Cell-phone population rate in Japan has been increased rapidly and handling various data communication such as voice, video, control etc. becomes very important. This demands to achieve passive device working over two GHz bands for next generation mobile phone. BAW(Bulk Acoustic Wave) resonator can be a promising device because it has been studied in the industrial field. When it is used as a filter device, BAW has spurious modes which cause a ripple in Passband.

This paper concerns with BAW resonator spurious suppression by using FEM commercial software, COMSOL Multiphysics 4.3b. It was found that the optimized shape of the border-framed electrode of BAW could remove the spurious modes and it was due to lateral wave attenuation along the surface of the electrode.

**Keywords:** BAW, spurious mode suppression, border-frame technique, COMSOL Multiphysics

## 1. Introduction

Cell-phone population rate in Japan has been increased rapidly[1] and we need to handle various data communication such as voice, video, control etc. This demands to achieve passive device working over two GHz bands for next generation mobile phone[2]. BAW(Bulk Acoustic Wave) resonators which can be connected to frequency selective filters on a chip are promising components for wireless communication systems. To meet the narrow band gap, there are still great demands for BAW filters and duplexers and improvement of resonator performances such as $Q$-factor and $k_t^2$(electro-mechanical coupling coefficients) is necessary. As we know, $k_t^2$ can be increased by getting large frequency difference between resonance mode and anti-resonance mode of BAW.

The BAW generators mainly utilize longitudinal acoustic waves and lateral acoustic waves which lead to spurious resonances. Various methods such as apodization, thickened border frame and air-edge reflector for spurious resonance suppression are discussed in current literatures[3].

In this paper, a kind of thickened border frame technique for spurious resonance suppression of BAW is examined numerically based on finite-element analysis. For the purpose COMSOL Multiphysics Ver.4.3b[4], commercial finite-element analysis software, is utilized here.

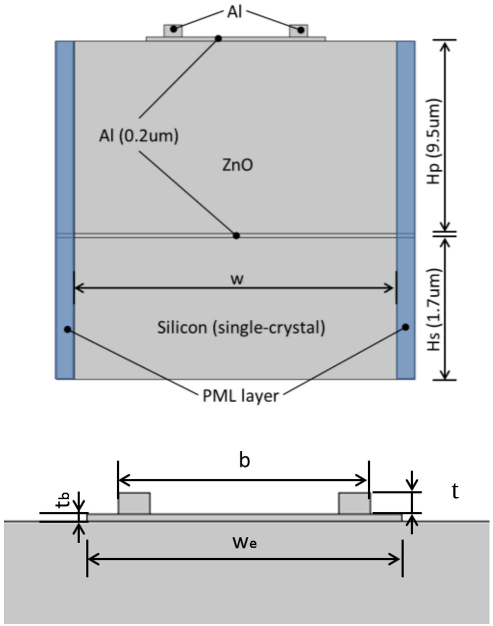

Figure 1 Analysis model: b is varied from200um to 500um, and border thickness t is varied from 0.2um to 0.6um. The base thickness of electrode tb and the width We are fixed to 0.2um and 500um, respectively. This figure shows a border-framed electrode. Flat electrode takes t=0 while the rest parts are hold same configuration as this figure.

Figure 1 shows the model considered here. Two-dimensional Al-ZnO-Al sandwich structure of BAW is assumed. They are mounted on the substrate of Si anisotropic single crystal. The geometrical configuration and material properties are designed to compare with the results of finite-element analysis of current literature[5]. An adjustable electrode which has a border frame of Al is attached on the top electrode for the purpose to examine its effect on suppression of spurious resonator. In order to optimize the electrode, the space b is reduced from 500um to 200um, and the thickness t is increased from 0.2um to 0.6um.

By using COMSOL Multiphysics Ver.4.3b, structural deformation and resonance performance such as admittance curve of this model configuration are examined.

## 3. Computational procedures

Two-dimensional model of BAW resonator is treated here. For the electrodes of Al, a linear elastic structural material and electric conductor is assumed. As a piezoelectric material for BAW resonator, ZnO is selected. In order to obtain the numerical solution of the linear elastic solid mechanics coupled with the piezoelectric materials, we used the Piezoelectric Device interface of the Solid Mechanics Engineering module of COMSOL Multiphysics. Numerical solution was obtained in frequency domain so that we could use complex number.

Constitutive relations of piezoelectric material for solid mechanics simulation are as follows:

The strain-charged form:

$$\begin{aligned}\mathbf{S} &= s_E\mathbf{T} + d^T\mathbf{E}\\ \mathbf{D} &= d\mathbf{T} + \varepsilon_T\mathbf{E}\end{aligned} \quad ,$$

or The stress-charged form:

$$\begin{aligned}\mathbf{T} &= c_E\mathbf{S} - e^T\mathbf{E}\\ \mathbf{D} &= e\mathbf{S} + \varepsilon_S\mathbf{E}\end{aligned} \quad .$$

Here, **S** is the strain, **T** is the stress, **E** is the electric field, and **D** is the electric displacement field. The material parameter $s_E$, $d$, and $\varepsilon_T$, corresponds to the material compliance, the coupling properties and the permittivity. These quantities are tensors of rank 4, 3, and 2 respectively. The material properties, $c_E$, e, and $\varepsilon_S$ are related to $s_E$, $d$, and $\varepsilon_T$. In the Piezoelectric Device interface, the Voigt notation is used for the definition of these tensors, which is standard in the literature for piezoelectricity. These tensor used here can be referred in the Appendix. We assumed loss factors of 0.001 and 0.01 for $c_E$ and $\varepsilon_S$, respectively.

Mapped (structured type) mesh elements were utilized to resolve very thin layers of electrodes and BAW region.

## 4. Results and discussion

First, configuration with flat electrode (Fig.1) was studied to obtain admittance curve and the result was compared with ref. [5]. The agreement regarding to resonance frequencies including spurious ones was very good as shown in Fig.2.

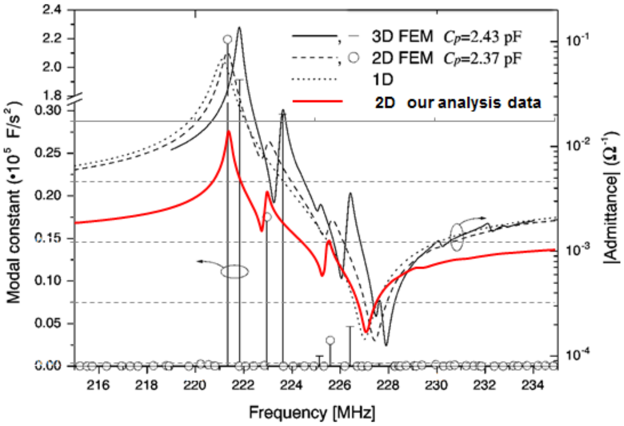

**Figure 2**. Validation result for admittance curve.

Then systematic study was executed for border-framed electrodes (Fig.1) having parametric geometry defined by us. The optimized shape was obtained as a result of extensive study shown in Fig.3. It was found that the resultant optimized shape has t=0.6um and b=500um, and it has no spurious frequencies as shown in Fig.3(b) (red colored solid line).

Since the current literature has not shown a distribution of the structural displacement, it has been examined here in detail. Figure 4 shows the vertical structural displacements along the surface of the top electrode whose frequency corresponds to resonance frequency fr, spurious frequencies fsp, and anti-resonance frequency fa.

Figure 4(a) shows the vertical displacement for the flat electrode in which large fluctuation of the vertical structural displacement can be observed. In figure 4(b), which is the result for the border-framed electrode, such fluctuations cannot be observed, and a plateau of the vertical displacement is appeared over the central region of the top electrode. Here, fr, fsp1, fsp2 and fa are 221.4MHz, 223.0MHz, 225.6MHz and 227.1MHz, respectively. Thus, we concluded the suppression mechanism of spurious modes by using the border-frame technique considered here was due to the attenuation of lateral wave, which can be observed in Fig.4.

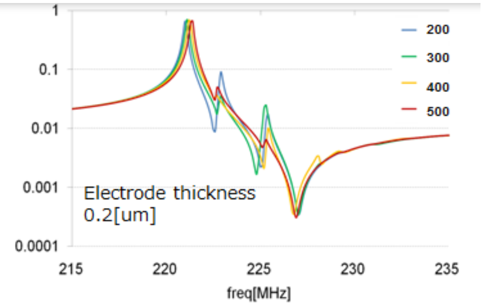

(a) Border-framed thickness t=0.2um

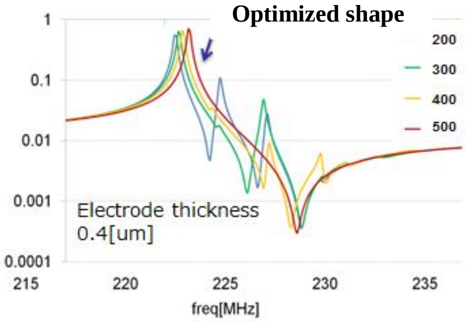

(b) Border-framed thickness t=0.4um

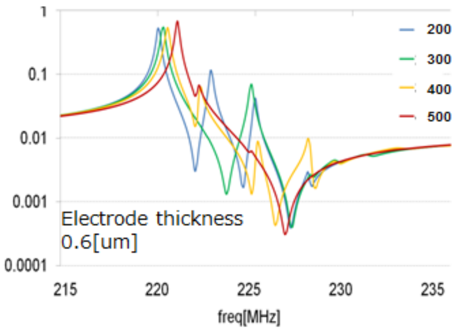

(c) Border-framed thickness t=0.6um

**Figure 3**. Systematic study for parameterized border-framed electrode geometries; the base thickness tb of the electrode is fixed to 0.2um, and the space b of the frame borders is changed to 200um, 300um, 400um, and 500um.

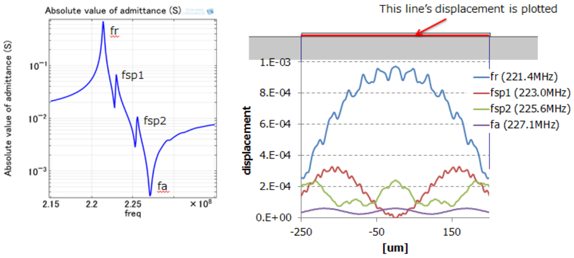

(a) Flat electrode

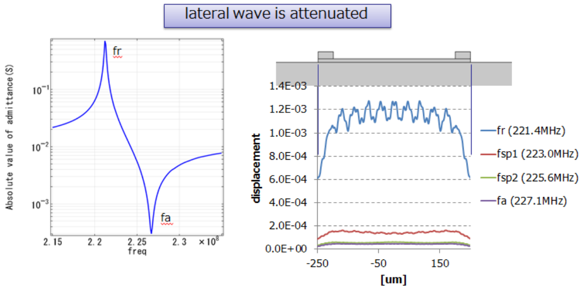

(b) Optimized border-framed electrode

**Figure 4**. Admittance curves and distributions of the vertical component of structural displacement along the surface of the top electrode.

## 5. Concluding remarks

We investigated the spurious mode suppression for the BAW resonator. The border-frame technique which has been proposed in many literatures is examined here numerically. It was found that the present finite-element analysis using COMSOL Multiphyiscs was validated via comparison with existing finite-element computation[5] for flat electrode, and that it could reproduce the suppression of the spurious modes by using the border-frame technique. Furthermore, the present study clarified by visualizing the structural vertical displacement of the top electrode surface that the suppression mechanism was due to the attenuation of the lateral wave along the surface of the top electrode.

Although the present study was conducted around 0.2GHz bands, it seems to be easy to apply the present method to the optimization of BAW resonator which is working in the RF region over two GHz bands. Through the present study, we found COMSOL Multiphyiscs is very useful design tool for BAW resonator.

## References

1. http://www.soumu.go.jp/menu_news/s-news/
2. T.Nishihara et al., IEEE Ultrasonics symposium, pp.969-972 (2002).
3. R.Aigner, "Bringing BAW Technology into Volume Production: The Ten commandments and the seven deadly sins," IEEE Int. Symp. Acoust. Wave. Dev. for Future Mobile Communication Syst.(2007).
4. For textbook, Roger W. Pryor, Multiphysics Modeling Using COMSOL 4: A First Principles Approach, Mercury Learning & Information(2012). For products, http://www.comsol.com/products/.
5. T.Makkonen et al., IEEE Trans. on Ultrasonics, Ferroelectrics, and Frequency Control, Vol.48, no.5 (2001).

## Acknowledgements

For this research the model "thin-film BAW resonator" in the Model library of COMSOL Multiphysics Ver.4.3b was great helpful. The authors would like to thank the entire technical team of COMSOL AB. Also we would like to thank Prof. Fujii of Chiba University for his helpful discussions.

## Appendix

$c_E$: Compliance matrix

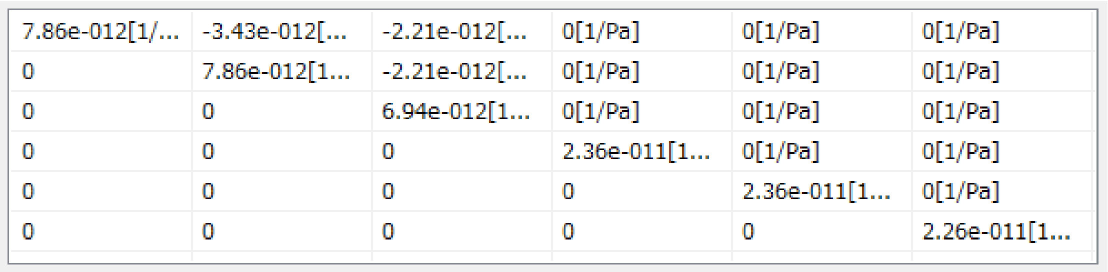

| | | | | | |
|---|---|---|---|---|---|
| 7.86e-012[1/... | -3.43e-012[... | -2.21e-012[... | 0[1/Pa] | 0[1/Pa] | 0[1/Pa] |
| 0 | 7.86e-012[1... | -2.21e-012[... | 0[1/Pa] | 0[1/Pa] | 0[1/Pa] |
| 0 | 0 | 6.94e-012[1... | 0[1/Pa] | 0[1/Pa] | 0[1/Pa] |
| 0 | 0 | 0 | 2.36e-011[1... | 0[1/Pa] | 0[1/Pa] |
| 0 | 0 | 0 | 0 | 2.36e-011[1... | 0[1/Pa] |
| 0 | 0 | 0 | 0 | 0 | 2.26e-011[1... |

$d$: Coupling matrix

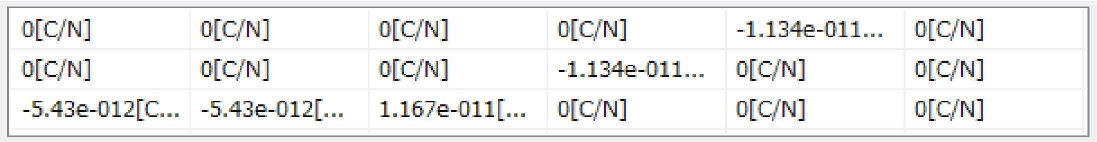

| | | | | | |
|---|---|---|---|---|---|
| 0[C/N] | 0[C/N] | 0[C/N] | 0[C/N] | -1.134e-011... | 0[C/N] |
| 0[C/N] | 0[C/N] | 0[C/N] | -1.134e-011... | 0[C/N] | 0[C/N] |
| -5.43e-012[C... | -5.43e-012[... | 1.167e-011[... | 0[C/N] | 0[C/N] | 0[C/N] |

$\varepsilon_T$: Relative permittivity matrix

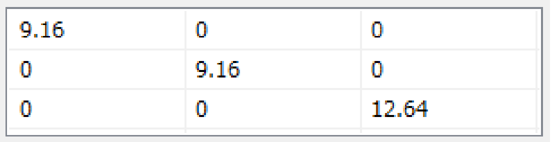

| | | |
|---|---|---|
| 9.16 | 0 | 0 |
| 0 | 9.16 | 0 |
| 0 | 0 | 12.64 |